Effect of Phase Behavior and Pressure on the Constant-Volume Heat Capacity and Intermolecular Interaction of CO_2 – Ethanol and CO_2 – *n*-Pentane Mixtures in the Critical Region

Hongping Li, Xiaogang Zhang, Buxing Han,* Jun Liu, Jun He, and Zhimin Liu[a]

Abstract: Study on the properties of the fluids near the critical point of mixed systems is a key for the development of supercritical (SC) technology and for the further understanding of the features of supercritical fluids (SCFs). The constant-volume molar heat capacity (C_v) of a solution is directly related to the internal energy, intermolecular interaction, and the microstructure of the solution. In this work, the C_v of CO_2 – *n*-pentane and CO_2 – ethanol systems was determined at 308.15 K in different phase regions. This work focuses on how the properties of the mixtures change with pressure, composition, and the structure of the components near the critical point of the mixtures. It was found that at fixed composition, a maximum in C_v versus pressure curve exists (C_v^{max}) that occurs at the pressure at which the isothermal compressibility (K_T) is the largest. We deduced that breaking the "clusters" in the SC mixtures is an endothermic process. It is very interesting that C_v increases sharply as the pressure approaches the critical point (CP) or bubble point (BP), while C_v is nearly independent of pressure and composition at the pressures well above the CP or BP pressure, and that the C_v at CP or BP can be several times larger than that at the high pressures. It can be deduced that at fixed composition the degree of "clustering" changes significantly with pressure near the CP or BP, and is the largest at CP and BP.

Keywords: critical region · heat capacity · molecular interactions · phase diagrams · supercritical fluids

Introduction

In recent years, scientists and engineers have paid more attention to supercritical fluids (SCFs).[1] Some are attracted by the unique properties of SCFs, while others are attracted by supercritical (SC) technologies. SCFs can be used in many processing applications, such as extraction and fractionation,[1a, 2] chemical reactions,[3] and material processing.[1a, 1b, 4] It is well known that some environmentally more acceptable SCFs, such as supercritical CO_2 and H_2O, can be used as solvents to replace organic solvents. On the other hand, SC technologies have many other advantages[1a, 1b, 2b] that will solve more challenging problems after our fundamental understanding of SCFs improves.

Generally, application systems are mixtures. In the recent published papers one can often find the phrases like "in the critical region" or "near the critical point". There may be two main reasons for this. First, the phase behavior of the application mixture is not known, although phase behavior is long-established field;[1c, 5] the other is that the properties of the mixture near the critical point differ significantly from those in other phase regions. Figure 1 shows a typical pressure versus composition phase diagram of a binary system at fixed temperature (T). X_1 is the mole fraction of the light component, C is the critical point, ABC is the bubble-point curve, and CDA is the dew-point curve. Generally, a mixture above the bubble-point curve can be regarded as a homogeneous subcritical fluid, a homogeneous mixture with $X_1 > X_C$ is considered as a vapor or SC mixture, while that at C is the critical mixture. The simple phase diagram of a binary system like that in Figure 1 has been used as an example in text books

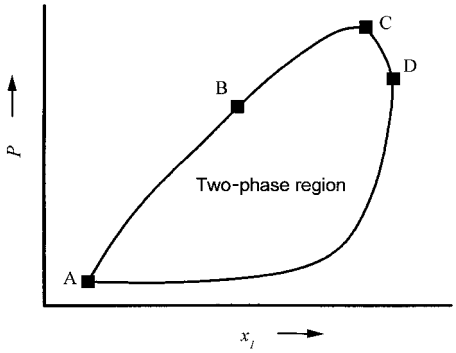

Figure 1. Phase diagram of binary system at constant temperature.

[a] Prof. B. Han, Dr. H. Li, Dr. X. Zhang, Dr. J. Liu, Dr. J. He, Dr. Z. Liu
Center for Molecular Sciences
Institute of Chemistry, the Chinese Academy of Sciences
Beijing 100080 (China)
Fax: (+86) 10-62559373
E-mail: hanbx@pplas.icas.ac.cn

  0947-6539/02/0802-0451 $ 17.50+.50/0

for many years. However, some very interesting questions should be studied further. For example, how do the properties of a homogenous subcritical fluid differ quantitatively from those of a supercritical fluid near the critical point? How does the structure of the components in the system affects the properties of the fluids near the critical point? Study on the properties of the fluids near the critical point is a key for the development of SC technologies and for further understanding of the features of SCFs, and researchers will pay more attention to this as SC technologies have become very attractive.

It is well known that constant-volume molar heat capacity (C_v) is directly related with the internal energy and intermolecular interaction in a system. The C_vs of some pure SCFs have been reported.[6] Kamilov et al[7] determined the C_v of an *n*-hexane – water mixture in a wide temperature range; they also studied the effect of temperature on C_v as the mixture passed liquid – liquid and liquid – vapor equilibrium regions. The constant pressure heat capacity (C_p) of some dilute SC mixtures has also been studied.[8]

In this work, we have built a calorimeter to determine the C_v of high-pressure mixtures and have studied CO_2 – *n*-pentane and CO_2 – ethanol binary mixtures at 308.15 K near the critical points of the mixtures. We focus on the effect of pressure on the C_v of the homogenous subcritical fluid, critical point fluid (with the critical composition), and supercritical fluid near the critical region of the mixtures, and the intermolecular interaction in different phase regions are also studied. A systematic study of the C_v of a mixture in different phase regions near the critical point was not found in a literature survey.

Experimental Section

Materials: CO_2 with a purity of 99.995% was supplied by the Beijing Analytical Instrument Factory. n-Pentane and ethanol were A.R. grade produced by Beijing Chemical Company. The chemicals were used without further purification

Calorimeter to determine C_v: The calorimeter was of the constant-temperature-environment type constructed in this laboratory. The principle of the apparatus was that the temperature of a constant-volume system will rise when the system is heated. The C_v could be calculated from the heat absorbed and the temperature increment. The schematic diagram of apparatus is shown in Figure 2. The calorimeter consisted of a calorimetric cell, a constant-temperature system, a high-pressure system, an electric-energy calibration system, and a data collecting and processing system.

The calorimetric cell was made of red copper, which was tested up to 16 MPa. The volume of the calorimetric cell was 73.00 mL, which was calibrated accurately by a gravimetric technique with water as the medium. Enamel covered constantan wire, which was wound tightly around the calorimeter cell, was used as a heater, and the resistance was $50.0 \pm 0.1\ \Omega$. The thermistor with a resistance of about 3 KΩ at 298.15 K was sealed into the wall of the calorimetric cell. In order to reduce the heat loss, the surface of the calorimeter cell was electroplated and covered by tinfoil paper. The temperature fluctuation of the water bath was less than ± 0.001 K of the desired temperature within 24 hours. A precision digital multimeter (Hewlett-Packard 34401A) was used to detect the temperature change. Using the multimeter, thermistor, and a computer, which was used to collect and process the experimental data, we could observe a temperature change of ± 0.00003 K. The constant current power was a model DP-981 with fine current adjustment of 0.01 mA, and the accuracy was $\pm 0.1\%$. The electronic timer was a model MJS/A, which was accurate to ± 0.001 s. Both of the constant current power and the electronic timer were produced by Beijing Tianchen Instrument Company.

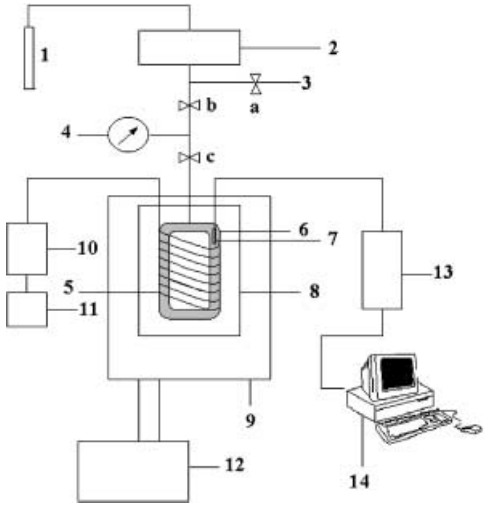

Figure 2. Schematic diagram of the calorimeter. 1: gas cylinder, 2: syringe pump, 3: outlet, 4: pressure gauge, 5: calibration heater, 6: calorimetric cell, 7: thermistor, 8: calorimetric outer shell, 9: constant temperature water bath, 10: constant current power, 11: timer, 12: pre-constant temperature bath, 13: precise digital multimeter, 14: on-line computer, a,b,c: valves.

The experiment began at the highest pressure. When the system reached thermal equilibrium, the resistance of the thermistor was recorded for five minutes by the computer. Then the constant current electric energy was supplied to heat the calorimetric cell for one minute. The temperature of the cell was recorded until final steady state was reached. In each experiment, the temperature increment ΔT was about 0.1 K and the heat leakage was corrected by using traditional methods.[9] The C_v of the fluid was calculated on the basis of the difference of energy equivalents[9] with and without the fluid in the calorimeter. The energy equivalent (ε) is given in Equation (1), in which I is the current supplied by constant current power, R is the resistance of heating coil, Δt is the time of the electric current, and $\Delta\theta_{corr}$ is the corrected temperature rise of the calorimeter.

$$\varepsilon = I^2 R \Delta t / \Delta\theta_{corr} \quad (1)$$

The corrected temperature rise $\Delta\theta_{corr}$ was obtained by extrapolating the initial and final periods in time-temperature curve.[9] After the experiment, some of the fluid in the system was released until the next desired pressure was reached, and the C_v at this pressure was determined as above. The composition of the fluid was not changed after the releasing process because there was only one phase in the system at the experimental conditions.

Apparatus and procedures to determine the phase behavior and critical point: The phase behaviors of the mixtures are the basis for selecting suitable conditions of C_v experiments. The apparatus and procedures for determining critical points and the phase behavior were the same as those described previously.[10] Very briefly, it consisted of a high-pressure optical cell, a constant temperature water bath, a pressure gauge, a temperature controller, and a thermometer. The high-pressure view cell was made of stainless steel with two borosilicate windows. The temperature of the water bath was controlled by a HAAKE D8 temperature controller ,and the temperature fluctuation of the water bath was ± 0.03 K. The accuracy of the temperature measurement was ± 0.05 K, The pressure gauge was composed of a pressure transducer (FOXBORO/ICT, Model 93) and an indicator, which was accurate to ± 0.025 MPa in the pressure range of 0 – 20 MPa. In a typical experiment, the apparatus was washed thoroughly with different solvents and dried under vacuum. The air in the system was evacuated, and a suitable amount of liquid chemical was charged by using a sample bomb. The gas was then charged by using a gas sample bomb. The mass of each chemical charged was known by the mass difference of the sample bomb before and after charging the system. The composition of the mixture in the system could be easily calculated from the masses of the chemicals. The water bath was maintained at desired temperature. After thermal equilibrium had been reached the piston in the optical cell was

0947-6539/02/0802-0452 $ 17.50+.50/0 *Chem. Eur. J.* **2002**, *8*, No. 2

moved up and down to change the volume or pressure of the system. The bubble point or critical point could be observed.[10] The density of the fluid could be obtained by the mass and volume of the mixture. In order to minimize the error originated from temperature and pressure measurements, we used the same pressure gauge and thermometer for phase behavior, density, and heat capacity measurements.

Results

Phase behavior: In this work we focus on how the C_v of CO_2–*n*-pentane and CO_2–ethanol binary mixtures changes with pressure and composition near the critical points. The phase behaviors of the systems are the basis for selecting suitable conditions. Thus, we first determined the critical points, bubble points, and the densities of the mixtures at 308.15 K, although phase behavior at other temperatures have been reported by other authors.[2b, 11]

Table 1 lists the bubble-point (BP) pressure, critical composition, and critical-point (CP) pressure at 308.15 K, and the results for CO_2–*n*-pentane system are also illustrated in Figure 3 (X_1 in the figure is the mole fraction of CO_2). The results calculated from the Peng–Robinson equation of state[12] (PR EOS) are also shown in the figure and agree well with the experimental data. For CO_2–ethanol system, the calculated values and the experimental results also agree well.

The critical composition of CO_2–*n*-pentane system at 308.15 K is $X_2 = 0.021$ (X_2 is the mole fraction of the second component, in this case pentane), and the critical pressure is 7.469 MPa (Table 1). Calculation of the critical temperature by using the Peng–Robinson equation of state shows that the critical temperature of the two binary systems increases with increasing X_2. Thus, the critical temperature of a CO_2–*n*-pentane mixture with $X_2 < 0.021$ is lower than 308.15 K. In other words, in Figure 3 a homogenous mixture is vapor or supercritical at the right-hand side of the critical composition; at the left-hand side of the critical composition, a mixture is compressed liquid or homogenous subucritical fluid when the pressure is higher than the bubble-point pressure. Similarly, the critical composition of CO_2–ethanol system at 308.15 K is $X_2 = 0.0203$, and any homogeneous mixture of $X_2 < 0.0203$ is vapor or supercritical fluid, and at $X_2 > 0.0203$ the mixture is compressed liquid or homogeneous subcritical fluid as pressure is higher than the bubble-point pressure. In this work we determined the C_v of some supercritical fluids, homogenous subcritical fluids, and critical fluids(with critical composition) near the critical region.

Table 1. Critical composition and bubble point pressure (BPP) of the CO_2–*n*-pentane and CO_2–ethanol systems at 308.15 K.

CO_2–*n*-pentane		CO_2–ethanol	
X_2	BPP [MPa]	X_2	BPP [MPa]
0.010	one phase[a]	0.010	one phase[a]
0.021[b]	7.469[b]	0.0203[b]	7.702[b]
0.050	7.169	0.050	7.438
0.100	6.524	0.084	7.157

[a] One phase in the whole pressure range. [b] Critical composition and critical pressure.

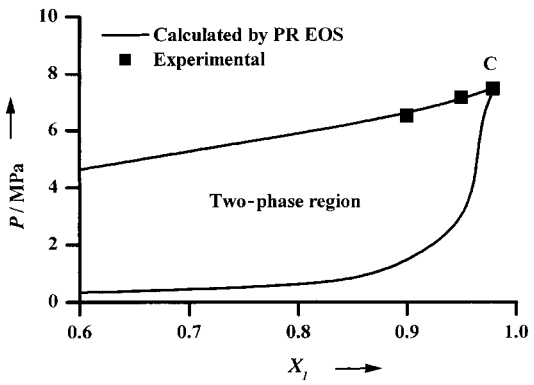

Figure 3. Phase diagram of the CO_2–*n*-pentane system.

Constant volume heat capacity of the fluids: Water may be the best substance for testing the reliability of our calorimeter because very accurate data are available in the literature.[13] Thus, the reliability of the calorimeter was first tested by measuring the C_v of water. The data determined in this work agree well with the literature values,[13] as can be seen from Table 2. It should be pointed out that the accuracy of the experiments for SCFs should be lower, especially in critical region because their densities are sensitive to temperature and pressure, and the experiments have to be carried out at high pressures.

Table 2. C_v [10^3 J kg^{-1} K^{-1}] of water at 308.15 K determined in this work and reported in literature.

1	2	3	Average value	Literature[a]
4.172	4.178	4.186	4.179	4.1782

[a] Ref. [13].

The C_v data of pure CO_2 at 308.15 K and different pressures determined in this work by four independent series of experiments are shown in Figure 4, which indicates that the reproducibility is better than ±1%. The reproducibility is good considering the fact that experiments were carried out at high pressure and in the critical region of CO_2. The published C_v data for CO_2 have been critically reviewed by Angus et al.[6b] Of these data, those by Amirkhanov et al.[6a] were perhaps the most comprehensive. The data reported by

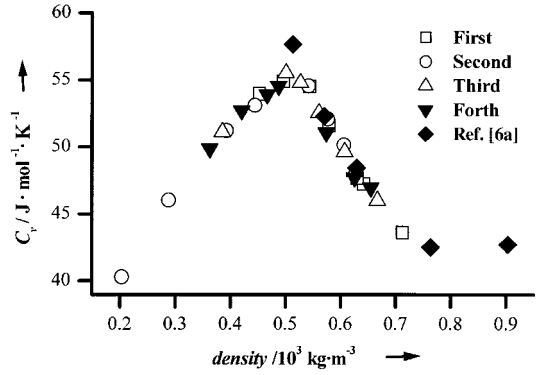

Figure 4. Dependence of the C_v of pure CO_2 on density determined in this work by a series of four independent experiments and comparison with reference values.

Amirkhanov et al.[6a] are also shown in the figure. It can be seen from Figure 4 that at the higher pressures our data agree well with the literature values within the experimental error. The deviation, however, is larger than the experimental error of this work and can be as large as 5 % near the critical density. The reason is that the density of CO_2 near the critical density is very sensitive to temperature and pressure; this makes obtaining accurate results difficult because the limitation of the pressure gauges.

On the basis of the determined results of the phase behavior, we selected some typical compositions and pressures in different phase regions for C_v studies. For CO_2–*n*-pentane system, the mixtures with $X_2 = 0.01$, 0.021, 0.05, and 0.1 were studied, and for CO_2–ethanol system $X_2 = 0.01$, 0.0203, 0.05, and 0.084 were selected. The values of C_v at different conditions are listed in Tables 3 and 4. Figures 5 and 6 illustrate the dependence of C_v of pure CO_2, CO_2–*n*-pentane, and CO_2–ethanol mixtures on pressure and composition at 308.15 K.

Isothermal compressibility of the fluids: The isothermal compressibility (K_T) of a fluid is an important characteristic parameter related with the solution structure.[14] The K_T of the fluids was calculated by using the density data determined in this work and the following well-known equation [Eq. (2)], in which ρ is the density of fluids.

$$K_T = \frac{1}{\rho}\left(\frac{\partial \rho}{\partial P}\right)_T \quad (2)$$

The variations of K_T with pressure for the two systems are shown in Figures 7 and 8, respectively.

Table 3. The constant-volume molar heat capacity (C_v) of CO_2–*n*-pentane binary mixtures at 308.15 K and different pressures.

$X_2 = 0.01$		$X_2 = 0.021$		$X_2 = 0.05$		$X_2 = 0.1$	
P [MPa]	C_v [J mol^{-1} K^{-1}]	P [MPa]	C_v [J mol^{-1} K^{-1}]	P [MPa]	C_v [J mol^{-1} K^{-1}]	P [MPa]	C_v [J mol^{-1} K^{-1}]
12.10	44.2	12.02	42.5	12.07	45.8	11.82	50.0
10.60	45.6	10.35	44.4	11.01	45.9	10.52	50.3
10.02	46.2	9.553	44.4	10.02	46.4	9.423	50.9
9.120	48.3	8.820	44.8	9.079	47.0	8.479	51.1
8.833	48.9	8.529	46.1	8.627	47.5	8.087	51.2
8.540	50.4	8.355	46.8	8.373	48.0	7.749	51.8
8.415	51.8	8.258	48.1	8.131	48.6	7.484	52.2
8.369	52.5	8.175	48.0	7.984	48.9	7.237	52.0
8.311	52.8	8.117	48.7	7.843	48.9	7.022	52.5
8.261	54.1	8.064	48.4	7.725	49.4	6.883	52.8
8.208	55.7	7.998	50.4	7.599	50.1	6.772	52.9
8.173	56.3	7.949	50.6	7.507	50.5	6.671	53.0
8.125	58.1	7.913	50.7	7.446	51.1	6.640	53.2
8.052	61.8	7.846	51.5	7.384	52.0	6.627	64.6
8.019	63.1	7.808	52.7	7.334	51.9	6.616	76.9
7.973	64.9	7.766	53.5	7.278	55.4	6.586	81.9
7.925	64.4	7.688	56.4	7.257	75.2	6.524	84.5
7.852	59.2	7.640	60.6	7.237	83.4		
7.800	56.1	7.596	72.3	7.198	90.8		
7.595	51.5	7.561	89.4	7.169	93.8		
7.397	49.9	75.22	93.3				
7.209	48.2	7.469	102.2				

Table 4. The constant-volume molar heat capacity (C_v) of CO_2–ethanol binary mixtures at 308.15 K and different pressures.

$X_2 = 0.01$		$X_2 = 0.0203$		$X_2 = 0.05$		$X_2 = 0.084$	
P [MPa]	C_v [J mol^{-1} K^{-1}]	P [MPa]	C_v [J mol^{-1} K^{-1}]	P [MPa]	C_v [J mol^{-1} K^{-1}]	P [MPa]	C_v [J mol^{-1} K^{-1}]
10.56	44.4	10.08	44.2	9.126	42.2	8.370	45.4
9.635	46.1	9.520	47.7	8.605	44.6	8.070	45.2
8.952	46.9	8.923	48.4	8.308	47.8	7.781	47.3
8.643	47.8	8.573	49.6	8.111	51.9	7.604	49.3
8.470	49.6	8.408	50.5	7.894	58.5	7.520	51.1
8.296	51.9	8.252	51.7	7.808	59.4	7.434	54.3
8.208	54.6	8.131	52.8	7.640	61.8	7.366	60.2
8.146	56.1	8.031	54.4	7.528	71.2	7.231	87.6
8.093	59.5	7.931	57.4	7.501	98.2	7.201	98.8
8.040	63.2	7.863	60.8	7.487	119.7	7.192	121.9
8.005	66.3	7.825	65.2	7.470	129.7	7.185	163.9
7.969	71.3	7.802	69.0	7.451	130.6	7.169	172.4
7.937	75.1	7.772	84.3	7.438	132.2	7.157	174.2
7.881	77.9	7.758	92.6				
7.834	74.3	7.731	111.4				
7.740	66.3	7.702	116.4				
7.669	60.2						
7.460	55.8						

0947-6539/02/0802-0454 $ 17.50+.50/0 *Chem. Eur. J.* **2002**, *8*, No. 2

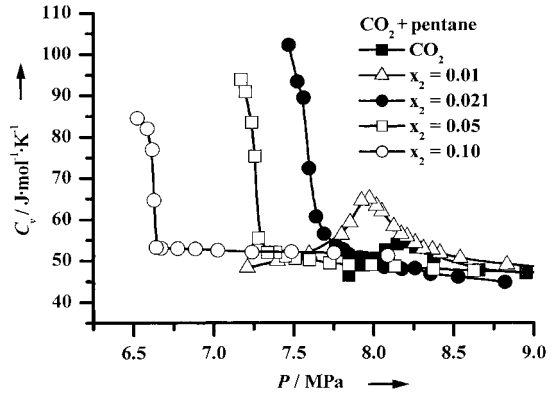

Figure 5. Dependence of the C_v of pure CO_2 and CO_2–*n*-pentane mixtures on pressure.

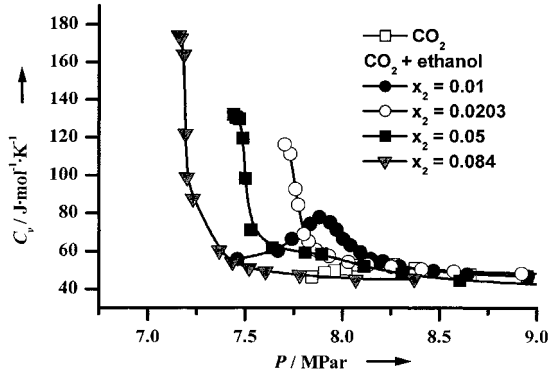

Figure 6. Dependence of the C_v of pure CO_2 and CO_2–ethanol mixtures on pressure.

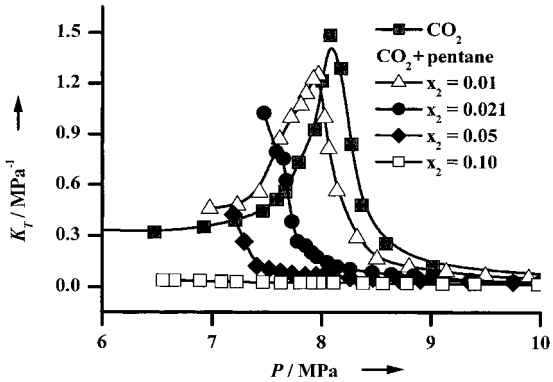

Figure 7. Isothermal compressibility of pure CO_2 and CO_2–*n*-pentane mixtures.

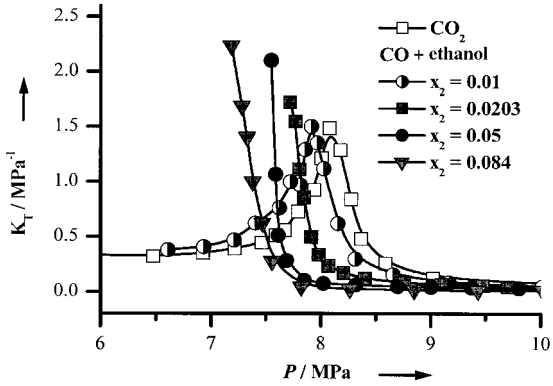

Figure 8. Isothermal compressibility of pure CO_2 and CO_2–ethanol mixtures.

Discussion

Vapor or supercritical fluids: Extensive experimental and theoretical studies of dilute SC solutions have shown that a local density enhancement or local composition enhancement exists in a highly compressible region;[1b, 14, 15] this is often referred to as "clustering" or aggregation between molecules. In this work, we used the words "clustering" or "cluster" to describe the local density enhancement or local composition enhancement. It should be emphasized that the clustering is a dynamic process, and the cluster members exchange with those in the bulk. In the systems studied in this work, the clustering is very complex. CO_2–CO_2, CO_2–solute, and solute–solute clusters may exist. The clustering is not significant at high pressures at which the compressibility of the fluids is small.

The critical temperatures of pure CO_2 and the solutions of $X_2 = 0.01$ are lower than 308.15 K for both systems studied, and there is only one phase in the systems in the concentration range of $X_2 = 0$–0.01, that is, either a vapor or supercritical phase. Figures 5 to 8 show that a maximum in each C_v versus pressure curve exists; these maxima corresponds to the largest K_T. One possible rationalization is that at the largest K_T less work is required to move the molecules closer, and the fluids have enough free volume. As a result, the attractive forces can move molecules into energetically favorable locations, and the degree of clustering is large. Thus more "clusters" are broken as temperature rises, and more heat is required for the same temperature increment. From the analysis above we can deduce that breaking the "clusters" in the supercritical fluids is an endothermic process.

Critical and subcritical fluids: As discussed above, we conducted the experiments at 308.15 K. Here, critical fluid means that a fluid has critical composition and a pressure higher than the critical pressure. Homogenous subcritical fluids are the fluids above the bubble-point curve, as shown in Figure 3. In this work, the pressure was carefully controlled so that the mixtures were in single phase regions.

Comparing the results in Table 1 and in Figures 5 and 6, we discover an interesting phenomenon. C_v is very sensitive to pressure near the critical point (CP) or the bubble point (BP), and increases sharply as the pressure approaches the critical or bubble point. The C_v at CP or BP can be several times larger than that at the high pressures at which the C_v is nearly independent of pressure. We can deduce that the degree of "clustering" changes significantly near the CP or BP and is the largest at CP and BP.

n-Pentane is a nonpolar compound, while ethanol is a strong polar compound. Comparing Figures 5 and 6, one can observe another interesting phenomenon. The variation of the maximum value in C_v curves (C_v^{max}) with X_2 is different for the two systems. For the CO_2–*n*-pentane system C_v^{max} increases with increasing X_2, as long as X_2 is smaller than the critical composition ($X_2 = 0.021$), and then decreases, that is, the C_v^{max} at the critical point is the largest. For the CO_2–ethanol system, however, the C_v^{max} increases monotonously with increasing concentration of ethanol. This is discussed qualitatively in the following.

Figures 5 and 6 show that C_v of the two mixtures is nearly independent of pressure and X_2 in the high-pressure region. Thus, the change in C_v results mainly from the variation of the intermolecular interaction between the molecules in the mixture. For CO_2–*n*-pentane system C_v^{max} at the critical point is the largest. It can be deduced that in the nonpolar mixture, the degree of clustering at the critical point is the largest.

The intermolecular interaction in CO_2–ethanol system is more complex. For example, some strong polar solutes can form hydrogen bonds in SCFs even when the concentration of the solutes is very low.[16] It can be expected that hydrogen bond between ethanol molecules exists in CO_2–ethanol system at the conditions studied in this work. CO_2 can act as a weak Lewis acid[17] and an interaction between the quadrupole of CO_2 and the dipole of ethanol may exist. It is very difficult to explain precisely why the C_v^{max} increases with increasing X_2 in the whole concentration range studied, while the C_v at high pressure is nearly independent of the composition and pressure. There are several possible reasons. First, the degree of hydrogen bonding and/or the quadrupole–dipole interaction increases sharply as pressure approaches CP or BP, and the number of the hydrogen-bonded species increases with the concentration of ethanol. More hydrogen bonds are broken as temperature rises when more hydrogen-bonded species exist in the system, and breaking hydrogen bonds is an endothermic process. The other possible reason may be that the degree of "clustering" at CP or BP reaches maximum at fixed composition and increases with increasing X_2. In other words, the polar compound enhances the "clustering" at CP or BP.

Acknowledgement

The authors are grateful to the Ministry of Science and Technology of China (G2000048010), the National Natural Science Foundation of China, and the Chinese Academy of Sciences for the financial support.

[1] a) M. A. McHugh, V. J. Kukonis, *Supercritical Fluid Extraction*, 2nd ed., Butterworth–Heinmann, Boston, **1994**; b) C. A. Eckert, B. L. Knutson, P. G. Debenedetti, *Nature* **1996**, *383*, 313–318; c) J. Ke, B. X. Han, M. W. George, H. K. Yan, M. Poliakoff, *J. Am. Chem. Soc.* **2001**, *123*, 3661–3670.

[2] a) G. Brunner, *Gas Extraction: An Introduction to Fundamentals of Supercritical Fluids and their Application to Separation Processes*, Steinkopff Darmstadt, New York, **1994**; b) "Supercritical Fluid Science: Fundamentals and Applications": *ACS Symp. Ser.* **1993**, *514*, whole volume.

[3] a) P. G. Jessop, W. Leitner, *Chemical Synthesis using Supercritical Fluids*, Wiley-VCH, Weinheim, **1999**; b) A Darr, M. Poliakoff, *Chem. Rev.* **1999**, *99*, 495–541; c) O. Kajimoto, *Chem. Rev.* **1999**, *99*, 355–389; d) J. F. Brennecke, J. E. Chateauneuf, *Chem. Rev.* **1999**, *99*, 433–452; e) P. G. Jessop, T. Ikariya, R. Noyori, *Chem. Rev.* **1999**, *99*, 475–493.

[4] A. Benedetti, A. Bertucco, P. Pallado, *Biotechnol. Bioeng.* **1997**, *53*, 232–241.

[5] a) G. M. Schneider, *Pure Appl. Chem.* **1983**, *55*, 479–492; b) C. P. Hicks, C. L. Young, *Chem. Rev.* **1975**, *75*, 119–175; c) M. L. McGlashan, *Pure. Appl. Chem*. **1985**, *57*, 89–103; d) B. A. Stradi, J. P. Kohn, M. A. Stadtherr, J. F. Brennecke, *J. Supercrit. Fluids* **1998**, *12*, 109–122; e) A. Kordikowski, D. G. Robertson, A. I. Aguiar-Ricardo, V. K. Popov, S. M. Howdle, M. Poliakoff, *J. Phys. Chem*. **1996**, *100*, 9522–9526.

[6] a) K. I. Amirkhanov, N. G. Polikhronidi, B. G. Alibekov, R. G. Batyrova, *Teploenergetika* **1971**, *18*, 59–62; b) A. Angus, B. Armstrong, K. M. Reuck, *International Thermodynamic Tables of the Fluid State Carbon Dioxide*, Pergamon, Oxford, **1976**.

[7] I. K. Kamilov, L. V. Malyshena, A. R. Rasulov, K. A. Shakbanov, G. V. Stipanov, *Fluid Phase Equilib.* **1996**, *125*, 177–184.

[8] J. R. Boulton, F. P. Stein, *Fluid Phase Equilib.* **1993**, *91*, 159–176.

[9] F. D. Rossini, *Experimental Thermochemistry*, Interscience, Wiley, New York, London, **1956**.

[10] H. F. Zhang, Z. M. Liu, B. X. Han, *J. Supercrit. Fluids* **2000**, *18*, 185–192.

[11] a) F. H. Poettmann, D. L. Katz, *Ind. Eng. Chem.* **1945**, *37*, 847–853; b) K. Suzuki, H. Sue, M. Itou, R. L. Smith, H. Inomata, K. Arai, S. Saito, *J. Chem. Eng. Data* **1990**, *35*, 63–66.

[12] D.-Y. Peng, D. B. Robinson, *Ind. Eng. Chem. Fundam*. **1976**, *15*, 59–64.

[13] R. C. Weast, *CRC Handbook of Chemistry and physics*, 66th ed., Boca Raton, Florida, **1985**.

[14] C. A. Eckert, D. H. Ziger, K. P. Johnston, S. Kim, *J. Phys. Chem.* **1986**, *90*, 2738–2746.

[15] a) S. C. Tucker, *Chem. Rev.* **1999**, *99*, 391–418; b) J. F. Brennecke, D. L. Tomasko, J. Peshkin, C. A. Eckert, *Ind. Eng. Chem. Res.* **1990**, *29*, 1682–1690; c) M. M. Maddox, G. Goodyear, S. C. Tucker, *J. Phys. Chem. B* **2000**, *104*, 6248–6257.

[16] a) S. G. Kazarian, R. B. Gupta, M. J. Clarke, K. P. Johnston, M. Poliakoff, *J. Am. Chem. Soc.* **1993**, *115*, 11099–11109; b) J. L. Fulton, G. G. Yee, R. D. Smith, *J. Am. Chem. Soc*. **1991**, *113*, 8327–8334; c) Q. Xu, B. X. Han, H. K. Yan, *J. Phys. Chem. A* **1999**, *103*, 5240–5245; d) K. Jie, S. Z. Jin, B. X. Han, H. K.Yan, D. Y. Shen, *J. Supercrit. Fluids* **1997**, *11*, 53–60.

[17] a) J. C. Meredith, K. P. Johnston, J. M. Seminario, S. G. Kazarian, C. A. Eckert, *J. Phys. Chem.* **1996**, *100*, 10837–10848; b) S. G. Kazarian, M. F. Vincent, F. V. Bright, C. L. Liotta, C. A. Eckert, *J. Am. Chem. Soc.* **1996**, *118*, 1729–1736.

Received: May 21, 2001 [F3275]

